UDC 681.586

# A ONE-DIMENSIONAL MATHEMATICAL MODEL OF PIEZOELECTRIC TRANSFORMERS FOR CAD SYSTEM

## Volodymyr Medvid; Iryna Belyakova; Olena Maruschak; Vadim Piscio

*Ternopil Ivan Puluj National Technical University, Ternopil, Ukraine,*

***Summary.*** *The model of a piezoelectric transformer (PT), which is more convenient for modeling in comparison with those, which are widely used in practice, is presented in this paper. Moreover, the proposed model can be directly applied in developing radio-electronic equipment and integrated into computer-aided design systems (CAD). The given model of piezoelectric transformer considers not only one but several harmonics and is simple for interactive change of parameters in the modeling process, as well as takes into account and changes the parameters of piezoelectric devices without leaving the basic CAD of radio-electronic equipment. The implementation of this model in the MicroCAP computer-aided design system is shown in the example. The results obtained during modeling are compared with experimental data.*

***Key words:*** *Equivalent circuit, piezoelectric transformer, a piezoelectric element, frequency harmonics, MicroCAP.*

**Statement of the problem.** One of the priorities in the development of control and ignition systems for gas-discharge lamps is the replacement of their electromagnetic components with piezoelectric transformers [1, 2]. As you know, the principle of operation of the piezoelectric transformer is as follows. When an alternating voltage is applied to the electrodes of the primary circuit of a piezoelectric transformer, mechanical vibrations occur due to the reverse piezoelectric effect. They are transmitted to other sections of the piezoelectric material, and due to the direct piezoelectric effect, causes a voltage change in the secondary circuit. In terms of their characteristics, piezoelectric transformers (PT) compare transformers with scattering, but they do not see magnetic fields and simplify the design. Therefore, the development of electronic devices based on a piezoelectric transducer remains very relevant.

**Analysis of the available investigations.** For modeling and calculation of piezoelectric transformers, the method of electromechanical analogies and methods of direct modeling by finite element methods are usually used. The method of electromechanical analogies is limited because it takes into account only one «working» electromechanical resonance of a piezoelectric transformer, rejecting all others. When modeling electrical circuits with a piezoelectric transformer, we must take into account the passage of harmonics of the input signal through this element. However, this is not possible, since the model approximates the frequency characteristics of PT only in the vicinity of the operating frequency.

In direct modeling of piezoelectric transformer, the finite element method is usually used [3–5], making it possible to obtain the dependencies between currents and stresses on the piezoelectric transformer with arbitrary accuracy. However, such models are quite complex and are not integrated into the radio-electronic equipment circuit modeling systems, and are separate complex systems [6–8].

Thus, a situation has arisen when a developer of electronic equipment either uses a simple model that does not take into account the passage of harmonics of the signal, or is forced

to use two CAD systems that are not integrated with each other at once, one for PT modeling, and the second for modeling the rest of the circuit [9–11]. In addition, high accuracy of the modeling results is usually not required, as the parameters of other circuit elements and materials have technological variation within the range of 2–10%.

**The Objective of the work.** The purpose of this article is to develop a model that takes into account the parameters of a piezoelectric device and not comes out of the basic electronic CAD. The developed model should, on the one hand, be acceptable in accuracy and take into account at least a few first harmonics (which is enough to perform practical tasks). On the other hand, it should be quite simple.

**Methods and the main assumptions in modeling.** To simplify the calculations, we will limit ourselves to the simplest one-dimensional model of a piezotransformer, which is quite accurate and is used to solve most practical problems. Within the framework of the model, we assume that the primary oscillations occur along the axis of the piezoelectric element. Suppose that forces, voltages, velocities, potentials and currents are represented as a Fourier transform:

$$f(t) = \frac{1}{\sqrt{2\pi}} \int_{-\infty}^{\infty} f(\omega) exp(j\omega t) dt . \tag{1}$$

At the same time, in all these cases, we omit the brackets to simplify and shorten the recording of dependencies. We will also describe the values of Fourier transforms, omitting the phrase «Fourier transform» to reduce the volume. To simulate a piezoelectric transformer, we conditionally divide it into sections of constant width, completely covered with electrodes and having a constant direction of polarization.

**Results. The section with transverse polarization.** Let the piezoelectric transformer Fig. 1 (a) have two sections with different polarization. Consider a section having a transverse polarization with the dimensions shown in Fig. 1 (b). Let's assume that the electrodes are placed on the upper and lower surfaces of the section so that the upper electrode of the $i$-th pair extends over the entire longitudinal of the upper surface of the plate and has a width of $b_i$ The lower electrode of the pair has the same location and occupies the lower surface of the plate. We will also assume that the gaps between different adjacent electrodes are close to zero, and the electrode system completely covers the entire surface of the piezoelectric element.
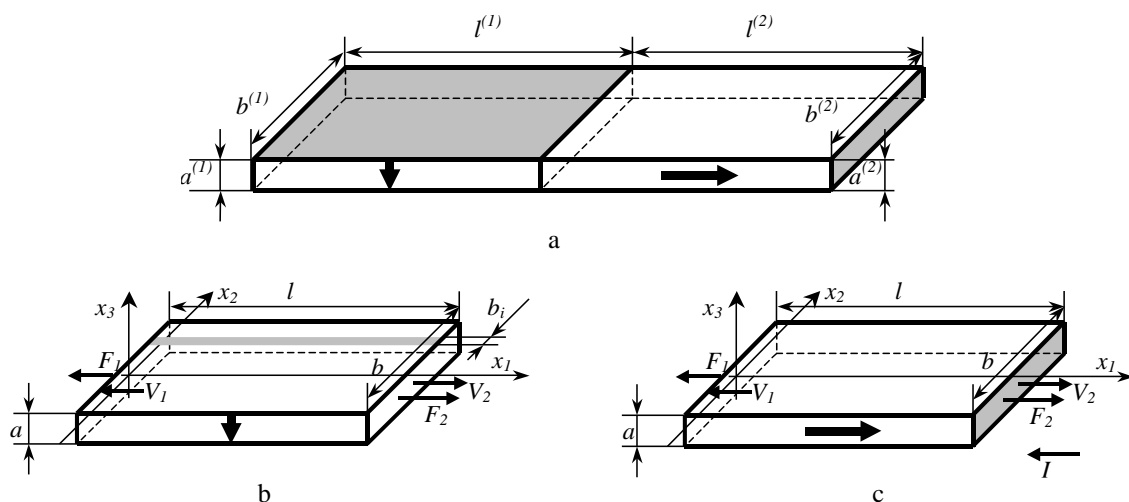


**Figure 1.** Piezotransformer a and its sections with transverse b and longitudinal c polarization

Let's also assume that external forces are acting on the right and left side of the section, causing the piezoelectric element to move at speeds $V_1$ and $V_2$, respectively, and the piezoelectric element design does not create forces on the upper, lower and side surfaces perpendicular to the axes $x_2$ and $x_3$. Then the equations of the piezoelectric medium state have the form [4]:

$$\hat{\varepsilon}_{11} = s_{11}\,\hat{\sigma}_{11} + s_{12}\,\hat{\sigma}_{22} + s_{13}\,\hat{\sigma}_{33} + d_{31}\,\hat{E}_3, \tag{2}$$

$$\hat{D}_3 = d_{31}\,\hat{\sigma}_{11} + d_{31}\,\hat{\sigma}_{22} + d_{33}\,\hat{\sigma}_{33} + \epsilon_{33}\,\hat{E}_3, \tag{3}$$

where $\hat{\xi}$ is the value depending on three coordinates. Since the speed of propagation of electromagnetic waves significantly exceeds the speed of vibrations in the material, a quasi-static approximation can be used for the electric field vector. Then the components of the electric field vector are represented by a potential:

$$\hat{E}_3 = -\frac{\partial\hat{\phi}}{\partial x_3}. \tag{4}$$

And the equation of motion of the medium has the form:

$$\frac{\partial\hat{\sigma}_{11}}{\partial x_1} + \frac{\partial\hat{\sigma}_{12}}{\partial x_2} + \frac{\partial\hat{\sigma}_{13}}{\partial x_3} - \rho\omega^2\,\hat{u}_1 = 0. \tag{5}$$

Using the zero approximation for thin beams and plates, which is widely used in solid mechanics, we assume stress $\hat{\sigma}_{22}$, $\hat{\sigma}_{33}$ values approximately equal to 0. Then the remaining normal component of stresses in the material will be determined as follows:

$$\hat{\sigma}_{11} = \frac{1}{s_{11}}\hat{\varepsilon}_{11} - \frac{d_{31}}{s_{11}}\hat{E}_3. \tag{6}$$

And the component $\hat{D}_3$ of the electric displacement is written as:

$$\hat{D}_3 = \frac{d_{31}}{s_{11}}\hat{\varepsilon}_{11} - \left(\epsilon_{33} - \frac{d_{31}^2}{s_{11}}\right)\frac{\partial\hat{\phi}}{\partial x_3}. \tag{7}$$

The actual distribution of stresses and deformations is unknown and generally depends on the coordinates $x_2$ and $x_3$, so we introduce the average values for the cross section of the plate and in the future we use such average values, which we denote without additional marks:

$$\xi_{ij} = \frac{1}{a\,b}\int\limits_{-a/2}^{a/2}\int\limits_{-b/2}^{b/2}\hat{\xi}_{ij}\,dx_2\,dx_3. \tag{8}$$

We will assume that the amount of displacement along the $x_1$ axis averaged over the surface of the electrode is equal to the amount of displacement averaged over the full cross section of the plate. That is, the equality is approximately fulfilled:

$$\frac{1}{a\,b_i}\int\limits_{-a/2}^{a/2}\int\limits_{S(b_i)}\hat{u}_1\,dx_2\,dx_3 \approx \frac{1}{a\,b}\int\limits_{-a/2}^{a/2}\int\limits_{-b/2}^{b/2}\hat{u}_1\,dx_2\,dx_3 = u_1, \tag{9}$$

where $\int\limits_{S(b_i)}...dx_2$ is the integral over the $i$-th electrodes pair width. Differentiating this expression by $x_1$, we get the approximate equality:

$$\varepsilon_{11} \approx \frac{1}{a\,b_i} \int\limits_{-a/2}^{a/2} \int\limits_{S(b_i)} \hat{\varepsilon}_{11} dx_2 dx_3. \tag{10}$$

By performing the averaging operation over the cross section of the state equation and taking into account the previously mentioned conditions for stresses, we obtain:

$$\sigma_{11} = \frac{\varepsilon_{11}}{s_{11}} + \frac{d_{31}}{s_{11}} \frac{\Delta\phi}{a}, \tag{11}$$

where $\Delta\phi = \frac{1}{b} \int\limits_{-b/2}^{b/2} \hat{\phi}\left(x_3 = \frac{a}{2}\right) - \hat{\phi}\left(x_3 = \frac{a}{2}\right) dx_2$ is the average width value of the potential difference between the upper and lower electrodes. If the electrode system is applied to the surface in such a way that the $i$-th upper and lower electrodes have a width $b_i$ and the potential difference between them is equal to $\Delta\phi_i$, then:

$$\Delta\phi = \frac{1}{b} \sum_i b_i\,\Delta\phi_i. \tag{12}$$

The component of the electric displacement vector averaged over the width of the $i$-th pair of electrodes is equal to:

$$D_3^{(i)} = \frac{d_{31}}{s_{11}} \varepsilon_{11} - \left(\epsilon_{33} - \frac{d_{31}^2}{s_{11}}\right) \frac{\Delta\phi_i}{a}. \tag{13}$$

Applying the averaging to the dynamics equation (5), we obtain a typical one-dimensional equation:

$$\frac{\partial \sigma_{11}}{\partial x_1} + \rho\omega^2\,u_1 = 0. \tag{14}$$

Without limiting generality, we can assume that at the boundaries $x_1 = 0$ and $x_2 = 0$, the velocity values ($v_1 = j\omega u_1$) are set having the direction shown in Fig. 1(a) and equal to $V_1$ and $V_2$, respectively. The equation (14), together with equation (11) and these boundary conditions, has a solution:

$$u_1 = -\frac{V_1 \sin\left(\sqrt{\rho\,s_{11}}\,\omega\,(l-x_1)\right)}{j\omega\,\sin\left(\sqrt{\rho\,s_{11}}\,\omega\,l\right)} + \frac{V_2 \sin\left(\sqrt{\rho\,s_{11}}\,\omega\,x_1\right)}{j\omega\,\sin\left(\sqrt{\rho\,s_{11}}\,\omega\,l\right)} \tag{15}$$

$$\sigma_{11} = \sqrt{\frac{\rho}{s_{11}}}\,\frac{\left(V_1 \cos\left(\sqrt{\rho\,s_{11}}\,\omega\,(l-x_1)\right) + V_2 \cos\left(\sqrt{\rho\,s_{11}}\,\omega\,x_1\right)\right)}{j\,\sin\left(\sqrt{\rho\,s_{11}}\,\omega\,l\right)} + \frac{d_{31}}{a\,b\,s_{11}} \sum_i b_i\,\Delta\phi_i. \tag{16}$$

And the component of the electrical displacement vector inside the $i$-th electrode is equal to:

$$D_3^{(i)} = \sqrt{\frac{\rho}{s_{11}}} \frac{d_{31}\left(V_1 \cos\left(\sqrt{\rho\, s_{11}}\,\omega\,(l-x_1)\right)+V_2 \cos\left(\sqrt{\rho\, s_{11}}\,\omega\, x_1\right)\right)}{j \sin\left(\sqrt{\rho\, s_{11}}\,\omega\, l\right)} + \left(\frac{d_{31}^{\,2}}{s_{11}} - \epsilon_{33}\right)\frac{\Delta\phi_i}{a}. \qquad (17)$$

The current flowing from the upper $i$-th electrode to the lower one is found as an integral:

$$I_i = -j\omega \int_0^l \int_{S(b_i)} D_3^{(i)} dx_2 dx_1 = -\frac{d_{31} b_i\,(V_1+V_2)}{s_{11}} - j\omega\left(\frac{d_{31}^{\,2}}{s_{11}} - \epsilon_{33}\right)\frac{b_i\, l\, \Delta\phi_i}{a}, \qquad (18)$$

where $S(b_i)$ is the cross-sectional area of the $i$-th electrode. The negative sign indicates the direction of current flow from the upper electrode to the lower one, that is, the opposite direction relative to the direction of the displacement vector. Taking into account the determination of average voltages, the forces generated by the piezoelectric element in the cross section is equal to:

$$F(x_1) = a b\, \sigma_{11} = a b \sqrt{\frac{\rho}{s_{11}}} \frac{\left(V_1 \cos\left(\sqrt{\rho\, s_{11}}\,\omega\,(l-x_1)\right)+V_2 \cos\left(\sqrt{\rho\, s_{11}}\,\omega\, x_1\right)\right)}{j \sin\left(\sqrt{\rho\, s_{11}}\,\omega\, l\right)} + \frac{d_{31}}{s_{11}}\sum_i b_i\,\Delta\phi_i. \qquad (19)$$

The force generated by the piezoelectric element in the cross-section at $x_1 = 0$ is:

$$F_1 = \sqrt{\frac{\rho}{s_{11}}} \frac{a b\left(V_1 \cos\left(\sqrt{\rho\, s_{11}}\,\omega\, l\right)+V_2\right)}{j \sin\left(\sqrt{\rho\, s_{11}}\,\omega\, l\right)} + \frac{d_{31}}{s_{11}}\sum_i b_i\,\Delta\phi_i \qquad (20)$$

and at $x_1 = l$ force is equal to:

$$F_2 = \sqrt{\frac{\rho}{s_{11}}} \frac{a b\left(V_1 + V_2 \cos\left(\sqrt{\rho\, s_{11}}\,\omega\, l\right)\right)}{j \sin\left(\sqrt{\rho\, s_{11}}\,\omega\, l\right)} + \frac{d_{31}}{s_{11}}\sum_i b_i\,\Delta\phi_i \qquad (21)$$

The schematic diagram simulating the last expression, taking into account the expression for current through all electrodes, is shown in the following figure (Fig 2(a)). Supposed that the voltage corresponds to the force at the boundary of the element, and the current simulates the velocity.
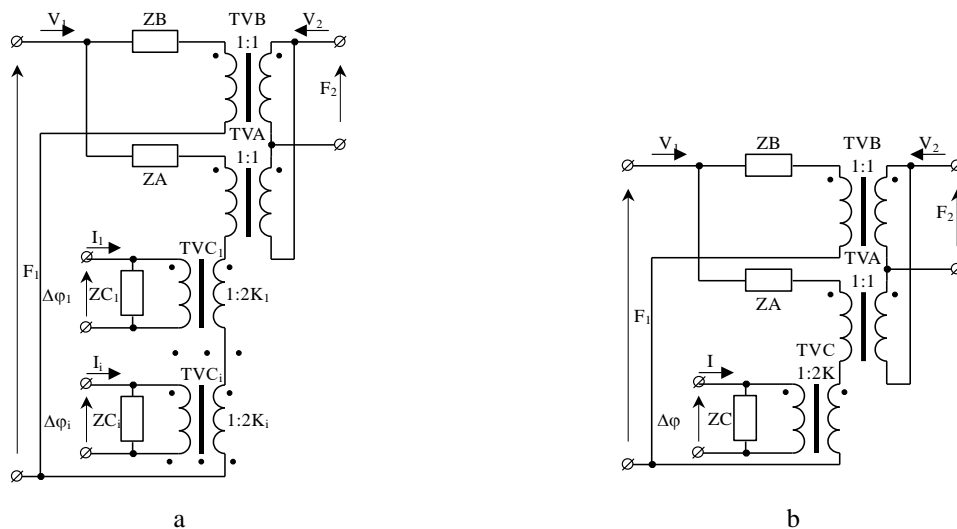


a

b

**Figure 2.** Schematic diagrams of the piezoelectric transformer section model with a transverse polarization, b longitudinal polarization

In this scheme, the transformers TVA and TVB have conversion coefficients equal in modulus 1, but their physical windings start opposite. The resistances ZA and ZB model the relationship between particle velocities and forces arising at the boundaries of the elements.

$$ZA = \sqrt{\frac{\rho}{s_{11}}} \frac{2ab\left(cos\left(\sqrt{\rho\,s_{11}}\,\omega\,l\right)+1\right)}{j\,sin\left(\sqrt{\rho\,s_{11}}\,\omega\,l\right)} = -j\,2ab\sqrt{\frac{\rho}{s_{11}}}\,ctg\left(\sqrt{\rho\,s_{11}}\,\omega\,l\,/\,2\right), \tag{22}$$

$$ZB = \sqrt{\frac{\rho}{s_{11}}} \frac{2\,ab\left(cos\left(\sqrt{\rho\,s_{11}}\,\omega\,l\right)-1\right)}{j\,sin\left(\sqrt{\rho\,s_{11}}\,\omega\,l\right)} = j\,2\,ab\sqrt{\frac{\rho}{s_{11}}}\,tg\left(\sqrt{\rho\,s_{11}}\,\omega\,l/2\right). \tag{23}$$

The transformers $TVC_i$ and resistances $ZC_i$ modeled electrodes through which oscillations are excited. The corresponding circuits are connected in series similarly to those shown for $TVC_1$ and $TVC_i$ transformers. The number of circuits coincides with the number of electrode pairs, and the electrode characteristics determine their parameters. Thus, the transformation coefficient $TVC_i$ is equal to $2K_i$ where $K_i = d_{31}b_i/s_{11}$. And the complex resistance associated with the $i$-th electrode is defined as:

$$ZC_i = \frac{1}{j\omega\frac{b_i\,l}{a}\left(\epsilon_{33} - \frac{d_{31}^{\,2}}{s_{11}}\right)} = \frac{a\,s_{11}}{j\omega\,b_i\,l\left(\epsilon_{33}s_{11} - d_{31}^{\,2}\right)}. \tag{24}$$

If only one pair of electrodes is on the surface, the value $b_1 = b$ is substituted in the formulas. Transcendental functions are inconvenient to use. For example, it is difficult to represent them in an equivalent electrical circuit, since not all CAD systems can use arbitrary expressions to calculate frequency-dependent resistances. Therefore, we decompose the transcendental functions $tg(x)$ and $ctg(x)$ into a series [5]:

$$tg(x) = \sum_{k=1}^{\infty}\frac{8x}{\pi^2(2k-1)^2 - 4x^2} = \sum_{k=1}^{\infty}\frac{8x}{\pi^2(2k-1)^2\left(1 - \frac{4x^2}{\pi^2(2k-1)^2}\right)}, \tag{25}$$

$$ctg(x) = \frac{1}{x} - \sum_{k=1}^{\infty}\frac{2x}{k^2\pi^2 - x^2} = \frac{1}{x} - \sum_{k=1}^{\infty}\frac{2x}{k^2\pi^2\left(1 - \frac{x^2}{k^2\pi^2}\right)}. \tag{26}$$

$$, ZA = \frac{4ab}{j\omega\,l\,s_{11}} + \sum_{k=1}^{\infty}\frac{j\omega\,2\rho\,abl}{k^2\pi^2\left(1 - \frac{\rho\,s_{11}\omega^2\,l^2}{4k^2\pi^2}\right)}, \tag{27}$$

$$ZB = \sum_{k=1}^{\infty}\frac{j\omega\,8\,\rho\,abl}{\pi^2(2k-1)^2\left(1 - \frac{\rho\,s_{11}\omega^2\,l^2}{\pi^2(2k-1)^2}\right)}. \tag{28}$$

**Representation of circuit resistances.**



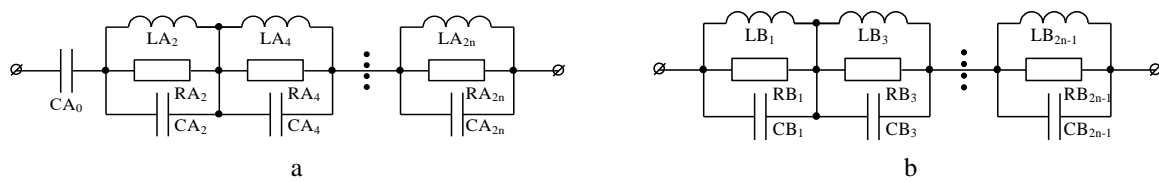a                                        b

**Figure 3.** Representation of resistance substitution scheme ZA a ZB b

Let's write down the representations of the complex resistances ZA, ZB, ZCi in the form of substitution schemes Fig. 3. It follows from the complex resistance formula that ZCi is a capacitance equal to:

$$CC_i = \frac{b_i \, l \left(\epsilon_{33} s_{11} - d_{31}^2\right)}{a \, s_{11}}. \tag{29}$$

The first term ZA, which is equal to $\dfrac{4\,a\,b}{j\omega\,l\,s_{11}}$, is the capacitance value $C_0 = \dfrac{s_{11}\,l}{4\,a\,b}$. It is also easy to prove that other members of ZA can be represented by series-connected parallel LC circuits with parameters:

$$LA_k = \frac{2\,a\,b\rho\,l}{k^2\pi^2}, \quad CA_k = \frac{s_{11}\,l}{8\,a\,b}. \tag{30}$$

To account for losses and Q – factor Q, we introduce loss resistances. As is known, the loss resistance included in parallel to a parallel resonant circuit is determined through the Q-factor of the circuit as follows:

$$RA_k = Q\sqrt{\frac{LA_k}{CA_k}} = \frac{4\,a\,b\,Q}{k\,\pi}\sqrt{\frac{\rho}{s_{11}}}. \tag{31}$$

Thus, the substitution scheme ZA can be represented in the form shown in Fig. 3a. In turn, ZB can also be described as series-connected parallel LC circuits. Comparing complex resistance of parallel LC circuit and ZB components, we get:

$$LB_k = \frac{8\,a\,b\,l\,\rho}{(2k-1)^2\pi^2}, \quad CB_k = \frac{s_{11}\,l}{8\,a\,b}. \tag{32}$$

Similarly introducing the losses resistance in the circuit, we get:

$$RB_k = Q\sqrt{\frac{LB_k}{CA_k}} = \frac{8\,a\,b\,Q}{(2k-1)\,\pi}\sqrt{\frac{\rho}{s_{11}}}. \tag{33}$$

Thus, the substitution scheme ZB can be represented in the form shown in Fig. 3(b).

**The section with longitudinal polarization.** Let's now consider the section with longitudinal polarization, with the dimensions shown in Fig. 1 (c). Suppose that the electrodes are located on the left and right side surfaces in such a way that the left and right electrodes are

stretched across the entire width and height of the plate and have width $b$ and height $a$. Let's also assume that external forces $F_1$, $F_2$ are acting on the right and left sides, causing the movement of PT with speeds $V_1$ and $V_2$. The design is made so that forces perpendicular to the axes do not act on the upper, lower and side surfaces of the piezoelectric element.

The equation of the piezoelectric medium state after the rotation of the indices of the material constants has the form [4]:

$$\hat{\varepsilon}_{11} = s_{13}\,\hat{\sigma}_{33} + s_{13}\,\hat{\sigma}_{22} + s_{33}\hat{\sigma}_{11} + d_{33}\hat{E}_1, \tag{34}$$

$$\hat{D}_1 = d_{31}\,\hat{\sigma}_{33} + d_{31}\,\hat{\sigma}_{22} + d_{33}\hat{\sigma}_{11} + \epsilon_{33}\hat{E}_1. \tag{35}$$

Similar to the previous case, quasi-static approximation for the electric field vector can be used. Therefore, the component of the electric field vector is represented by the potential according to the known formula:

$$\hat{E}_1 = -\frac{\partial\hat{\phi}}{\partial x_1}. \tag{36}$$

As in the previous case, assume that the stress values $\hat{\sigma}_{22}$, $\hat{\sigma}_{33}$ are approximately equal to 0. Then the stress component in the material is determined by deformations as follows:

$$\hat{\sigma}_{11} = \frac{1}{s_{33}}\hat{\varepsilon}_{11} + \frac{d_{33}}{s_{33}}\frac{\partial\hat{\varphi}}{\partial x_1} \tag{37}$$

And the component $\hat{D}_1$ of the electrical displacement vector is presented as follows:

$$\hat{D}_1 = \frac{d_{33}}{s_{33}}\hat{\varepsilon}_{11} - \left(\epsilon_{33} - \frac{d_{33}{}^2}{s_{33}}\right)\frac{\partial\hat{\phi}}{\partial x_1}. \tag{38}$$

We again introduce the average values for the cross-sectional area of the plate. By performing the averaging operation over the cross-section of the equation of state and taking into account the above conditions for stresses, we obtain:

$$\sigma_{11} = \frac{1}{s_{33}}\varepsilon_{11} + \frac{d_{33}}{s_{33}}\frac{\partial\phi}{\partial x_1}, \qquad D_1 = \frac{d_{33}}{s_{33}}\varepsilon_{11} - \left(\epsilon_{33} - \frac{d_{33}{}^2}{s_{33}}\right)\frac{\partial\phi}{\partial x_1}. \tag{39}$$

The electrodynamics equation relating the components of the electric displacement vector has the form:

$$\frac{\partial\hat{D}_1}{\partial x_1} + \frac{\partial\hat{D}_2}{\partial x_2} + \frac{\partial\hat{D}_3}{\partial x_3} = 0. \tag{40}$$

Averaging it over the cross-sectional area and taking into account that the electric displacements on the lateral, upper and lower surfaces are equal to 0, it can be shown that the equation after averaging will get the following form:

$$\frac{\partial D_1}{\partial x_1} = 0. \tag{41}$$

Thus the component $D_I$ is a constant over the variable $x_I$. And the current through the electrodes is equal to:

$$I = -j\omega \int_{-a/2}^{a/2} \int_{-b/2}^{b/2} D_I dx_2 dx_3 = j\omega\, a\, b\, D_I. \tag{42}$$

And, the derivative of the potential is equal to:

$$\frac{\partial\phi}{\partial x_I} = \frac{d_{33}}{\epsilon_{33}} \sigma_{11} + \frac{I}{j\omega\,\epsilon_{33}\,a\,b} \tag{43}$$

After averaging the medium dynamics equation, it takes the form:

$$u_I = -\frac{1}{\rho\omega^2}\frac{\partial\sigma_{11}}{\partial x_I}. \tag{44}$$

Again, we assume that at the boundaries $x_I = 0$ and $x_I = l$, the velocity values ($v_I = j\omega\,u_I$) are set, having the direction shown in Fig. 1(c) and equal to $V_I$ and $V_2$, respectively. Equation (44) together with equations (39) and this boundary conditions has the solution:

$$u_I = -\frac{V_I \sin(r(l - x_I))}{j\omega \sin(r\, l)} + \frac{V_2 \sin(r\, x_I)}{j\omega \sin(r\, l)}, \tag{45}$$

$$\sigma_{11} = \frac{\epsilon_{33} r(V_I \cos(r(l - x_I)) + V_2 \cos(r\, x_I))}{j\omega\left(\epsilon_{33}s_{33} - d_{33}^2\right)\sin(r\, l)} - \frac{d_{33}^2 (V_I + V_2)}{\left(\epsilon_{33}s_{33} - d_{33}^2\right)j\omega\, s_{33}\, l} + \frac{d_{33}}{l\, s_{33}}\Delta\phi., \tag{46}$$

$$I = j\omega\frac{a\, b}{l}\frac{\left(\epsilon_{33}s_{33} - d_{33}^2\right)}{s_{33}}\Delta\phi - \frac{a\, b}{l}\frac{d_{33}}{s_{33}}(V_2 + V_I) \tag{47}$$

where $\Delta\phi = \phi(l) - \phi(x0)$ potential difference between $x_I = 0$ and $x_I = l$, $r = \sqrt{\dfrac{\rho\left(\epsilon_{33}s_{33} - d_{33}^2\right)}{\epsilon_{33}}}\,\omega$.

Now, let us define the force generated by the piezoelectric element at the boundary $x_I = 0$. Taking into account the definition of average voltages and substituting the expression mentioned above for current into the formula, we get:

$$F_I = \frac{\epsilon_{33}\, a\, b}{\left(\epsilon_{33}s_{33} - d_{33}^2\right)j\omega\, l}\left(\left(\frac{rl\cos(rl)}{\sin(r\, l)} - \frac{d_{33}^2}{\epsilon_{33}s_{33}}\right)V_I + \left(\frac{rl}{\sin(r\, l)} - \frac{d_{33}^2}{\epsilon_{33}s_{33}}\right)V_2\right) + \frac{d_{33}}{s_{33}}\frac{a\, b}{l}\Delta\phi. \tag{48}$$

Similarly, the force created by the piezoelectric element at the boundary $x_I = l_I$ is equal to:

$$F_2 = \frac{\epsilon_{33}\, a\, b}{\left(\epsilon_{33}s_{33} - d_{33}^2\right)j\omega l}\left(\left(\frac{rl}{\sin(r\, l)} - \frac{d_{33}^2}{\epsilon_{33}\, s_{33}}\right)V_I + \left(\frac{rl\cos(r\, l)}{\sin(r\, l)} - \frac{d_{33}^2}{\epsilon_{33}\, s_{33}}\right)V_2\right) + \frac{d_{33}a\, b}{s_{33}\, l}\Delta\phi. \tag{49}$$

Let's construct the substitution scheme that models the last expressions, considering the expression for currents through all electrodes. We assume the voltage corresponds to the force

at the element boundary, and the current models the velocity of the particles. The substitution scheme for the section with longitudinal polarization has the form shown in Fig. 2 (b). Comparing Fig. 2(a) and Fig. 2(b), we see that the differences between them are minimal and are related to the number of TVC transformers and ZC resistances, but the components parameters are different. The resistances and transformation ratio is:

$$ ZA = \frac{2 \epsilon_{33} \, a \, b}{\left(\epsilon_{33} s_{33} - d_{33}^{2}\right) j \omega l} \left( rl \, ctg \left( r \, l/2 \right) - 2 \frac{d_{33}^{2}}{\epsilon_{33} \, s_{33}} \right), \tag{50} $$

$$ ZB = \frac{j \, 2 \, \epsilon_{33} \, a \, b \, r}{\left(\epsilon_{33} s_{33} - d_{33}^{2}\right) \omega} tg \left( rl/2 \right), \tag{51} $$

$$ ZC = \frac{l \, s_{33}}{j \omega \, a \, b \left(\epsilon_{33} s_{33} - d_{33}^{2}\right)}, \quad K = \frac{a \, b}{l} \frac{d_{33}}{s_{33}}. \tag{52} $$

It should be noted that, in contrast to the model given in [4], the given model has not negative resistances. Using the expansions of transcendental functions $ctg( x )$ and $tg( x )$ into rows [5], we get:

$$ ZA = \frac{4 \, a \, b}{j \omega \, l \, s_{33}} + \sum_{k=1}^{\infty} \frac{j \, 2 \, \omega \, a \, b \, \rho \, l}{k^{2} \pi^{2} \left( 1 - \frac{\rho \left(\epsilon_{33} s_{33} - d_{33}^{2}\right) \omega^{2} \, l^{2}}{4 \, \epsilon_{33} \, k^{2} \pi^{2}} \right)}, \tag{53} $$

$$ ZB = \sum_{k=1}^{\infty} \frac{j \, 8 \, a \, b \, \rho \, \omega \, l}{\pi^{2} ( 2k - 1 )^{2} \left( 1 - \frac{\rho \left(\epsilon_{33} s_{33} - d_{33}^{2}\right) \omega^{2} \, l^{2}}{\pi^{2} ( 2k - 1 )^{2} \epsilon_{33}} \right)}. \tag{54} $$

**Representation of circuit resistances.** Let us define the representation of complex resistances ZA, ZB, ZC in substitution electric circuits. From the formula of complex resistance, it follows that ZC is the capacitance value:

$$ CC = \frac{a \, b}{l} \frac{\left(\epsilon_{33} s_{33} - d_{33}^{2}\right)}{s_{33}}. \tag{55} $$

The substitution scheme for ZA ZB does not differ by structure from the section mentioned above (Fig. 3). The first term ZA, which is equal to $ZA_0 = 4 \, a \, b / j \, \omega \, l \, s_{33}$, is the capacitance value $C_0 = s_{33} \, l / 4 \, a \, b$. Other ZA terms are represented as series-connected parallel LC circuits with the values of inductors and capacitances:

$$ LA_k = \frac{2 \, a \, b \rho \, l}{k^{2} \pi^{2}}, \quad CA_k = \frac{\left(\epsilon_{33} s_{33} - d_{33}^{2}\right) l}{8 \, a \, b \, \epsilon_{33}}. \tag{56} $$

As in the previous case, we introduce loss resistances $RA_k$, which are determined by the quality factor:

$$ RA_k = Q \sqrt{\frac{LA_k}{CA_k}} = \frac{4 \, a \, b \, Q}{k \pi} \sqrt{\frac{\rho \, \epsilon_{33}}{\left(\epsilon_{33} s_{33} - d_{33}^{2}\right)}}. \tag{57} $$

The complex resistance ZB is represented as series-connected parallel LC circuits as well. Comparing the complex resistance of parallel LC circuit and ZB components, we get the values of inductances and capacitances of the circuits:

$$LB_k = \frac{8\,a\,b\,\rho\,l}{\pi^2\,(2k-1)^2}, \quad CB_k = \frac{\left(\epsilon_{33}s_{33} - d_{33}^2\right)l}{8\,a\,b\,\epsilon_{33}}. \tag{58}$$

As for the previous, let us introduce the loss resistance $RB_k$ by quality factor Q:

$$RB_k = Q\sqrt{\frac{LB_k}{CB_k}} = \frac{8\,a\,b\,Q}{(2k-1)\pi}\sqrt{\frac{\rho\,\epsilon_{33}}{s_{33}\epsilon_{33} - d_{33}^2}} \tag{59}$$

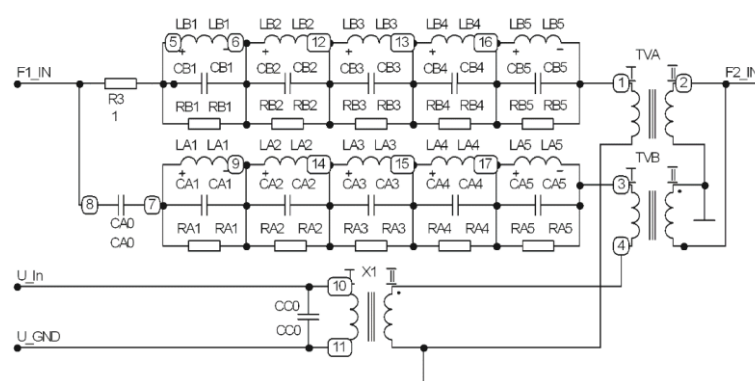**General model of cross-longitudinal type PT**



**Figure 4.** The structure of the piezoelectric section model

From the point of view of using CAD, it is advisable to give the user the opportunity to combine individual sections of the PT, presented as separate elements [12, 13]. In this case, each section together with its electrodes is described by a separate element. When modeling the structure, the terminals of the sections are connected, simulating the mechanical connection of the sections to each other as simple elements of electrical circuits [14, 15].

For example, let's construct the piezoelectric transformer substitution scheme consisting of two sections – with longitudinal and transverse polarization, respectively. At the sections boundary, the force and velocity coincide, so the corresponding contacts should be connected. The forces are equal to zero on the free boundaries of PT sections, which corresponds to the short circuit at the corresponding inputs. The scheme modeling separate section of the piezoelectric element is shown in Fig. 4.
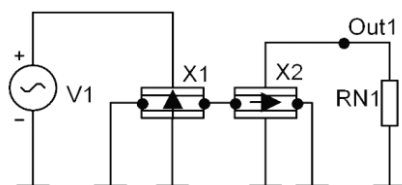


**Figure 5.** Graphical representation of the connection of piezoelectric transformer sections in the CAD
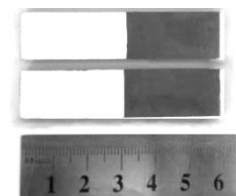


**Figure 6.** View of the modeled piezoelectric transformers and measured parameters

The use of sections as macronutrients to obtain a complete model of a piezoelectric converter is shown in Figure 5.
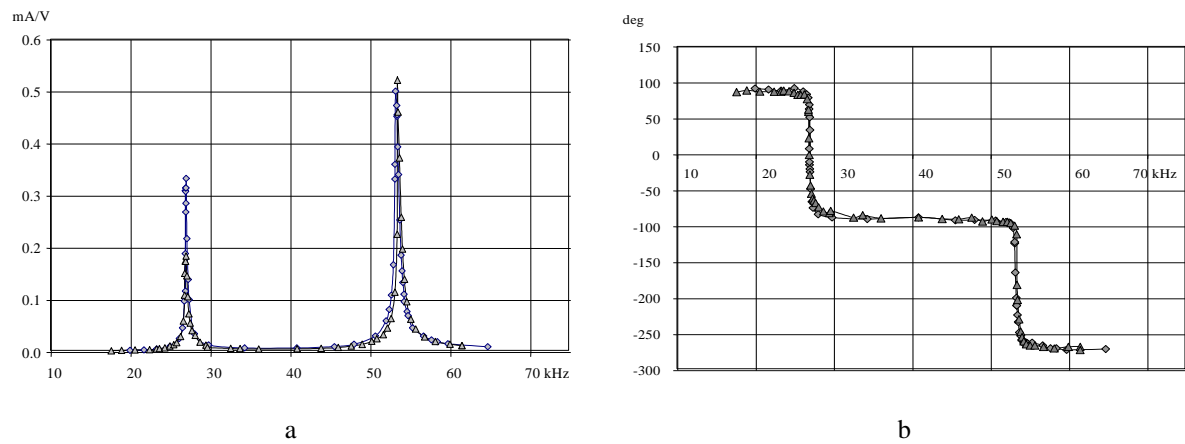
**Figure 7.** The transfer ratio for output current (mA) vs the input voltage (V):
a – amplitude, b – phase (measurement results)

We measured natural characteristics of piezoelectric transformers made of PZT-4 ceramics with geometric dimensions 60x14x3 mm (Fig. 6) to test the obtained model. The transfer ratio for output current (mA) vs the input voltage (V) shown in Fig 7.

The same piezoelectric transformer are modeled in MicroCap (Fig. 5.) During the modeling process, the frequency dependences of the output transfer current ratio on the input voltage amplitude at load resistance of 1 kOhm are obtained. The transfer ratio obtained in the simulation for the output current (mA) depending on the input voltage (V) is shown in Fig. 8.
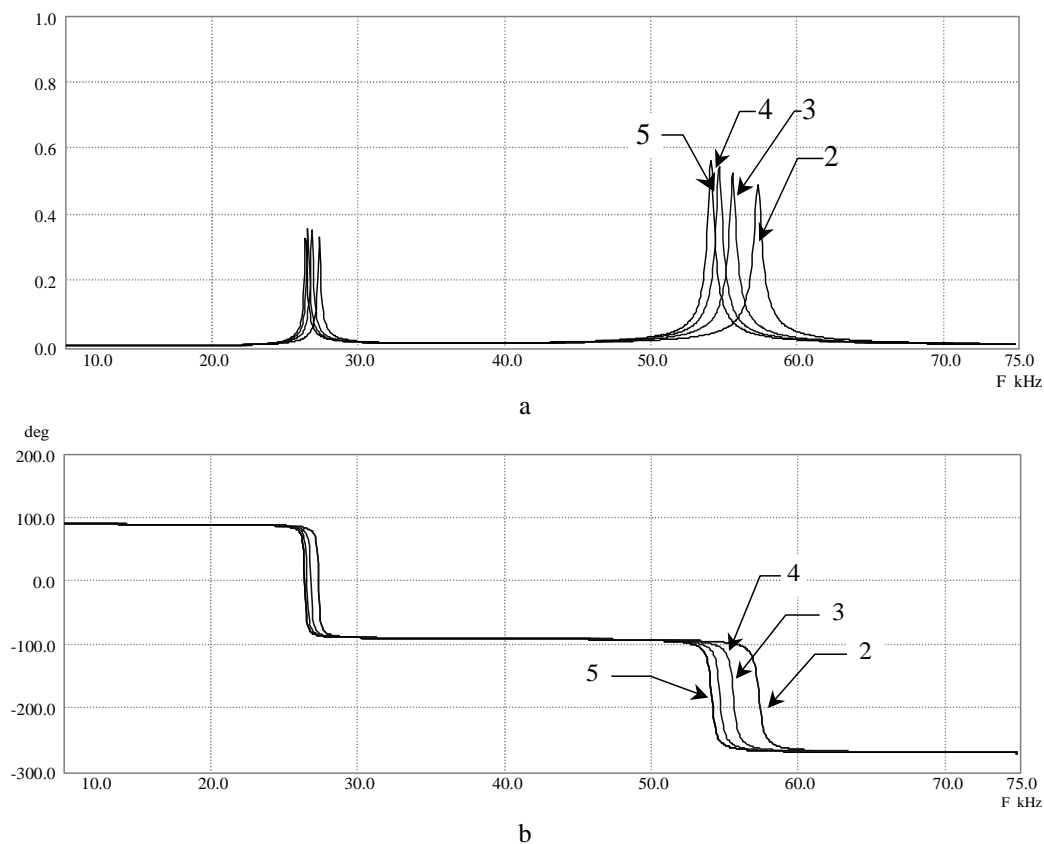


**Figure 8.** The transfer ratio for output current (mA) vs the input voltage (V): a - amplitude,
b – phase (modeling results)

The sufficient number of circuits in the model is determined by the number of circuits reduced by setting the resistance values RA5-RA3/RB5-RB3 equal to zero. Decoding of the graph's digital symbols is given in Table 1.

**Table 1**

Decoding of digital symbols

| Notation on the graph | Set off ZA resistance circuits | | | | | Set off ZB resistance circuits | | | | |
|---|---|---|---|---|---|---|---|---|---|---|
| | LA1/ CA1 | LA2/ CA2 | LA3/ CA3 | LA4/ CA4 | LA5/ CA5 | LB1/ CB1 | LB2/ CB2 | LB3/ CB3 | LB4/ CB4 | LB5/ CB5 |
| 2 | + | + | – | – | – | + | + | – | – | – |
| 3 | + | + | + | – | – | + | + | + | – | – |
| 4 | + | + | + | + | – | + | + | + | + | – |
| 5 | + | + | + | + | + | + | + | + | + | + |
| + – circuit involved in piezoelectric transformer section modeling; – – circuit excluded from piezoelectric transformer section modeling by setting the parallel active loss resistance to zero. | | | | | | | | | | |

It is evident that having two circuits in each complex resistance, the qualitative coincidence of experimental characteristics of piezoelectric transformer and those obtained from the model is observed, and having five circuits – not only qualitative but also quantitative coincidences are observed.

**Conclusions.** In contrast to the classical model, the proposed scheme and modeling method makes it possible to take into account the presence of sections with longitudinal or transverse polarization.

Based on the modeling mentioned above technique, the scheme modeling separate section of the piezoelectric element is proposed. The corresponding connection of such components can be used for obtaining the characteristics of piezoelectric transformers of different types.

The model makes it possible to create the piezoelectric transformer as a circuit consisting of standard blocks, simplifying the electrodes' location and coordination with the circuit. The proposed model considers any number of resonance and the presence of several electrodes located on the piezoelectric transformer.

It is possible to use CAD tools (for example, MicroCAP software) to model PT sections. For these reasons, each element with its electrodes is described by macro elements. Then, during the circuit modeling process, the section's output models mechanical vibrations as simple electrical circuits are connected.

**References**
1. Katz H. W. Solid state magnetic and dielectric devices. New York: Wiley, 1959. 542 p.
2. Lavrinenko V. V., P`ezoe`lektricheskie transformatory`. M.: E`nergiya, 1975. 112 p.
3. Yang Y. J., Chen C. C., Chen Y. M., et al., Modeling of piezoelectric transformers using finite-element technique. Journal of the Chinese Institute of Engineers. 2008. 31 (6). P. 925–932. https://doi.org/10.1080/02533839.2008.9671447
4. Yerofeev A.A., Danov G.A., Frolov V.N. Piezoelectric transformers and their application in electronics, Moscow: Radio i Sviaz (Radio and Communications), 1988, 128 p.

5. Harris J. W., Horst S. Handbook of mathematics and computational science. Springer Science & Business Media, 1998. https://doi.org/10.1007/978-1-4612-5317-4
6. Yerofeev A. A., Piezoelectronic automation devices. Leningrad: Mashinostroenie, 1982. 212 p.
7. Vazquez Carazo, A. Piezoelectric Transformers: An Historical Review. Actuators 2016, 5, 12. Doi: 10.3390/act5020012. https://doi.org/10.3390/act5020012
8. Ozeri S. and Shmilovitz D. Piezoelectric transformers model parameters extraction based on time domain measurements, Twenty-First Annual IEEE Applied Power Electronics Conference and Exposition, 2006. APEC '06., 2006. P. 5. Doi: 10.1109/APEC.2006.1620748.
9. Bronshtein S., Abramovitz A., Bronshtein A. and Katz I. A Method for Parameter Extraction of Piezoelectric Transformers. IEEE Transactions on Power Electronics. 2011. 26 (11). P. 3395–3401. https://doi.org/10.1109/TPEL.2011.2139225
10. Hsu Y., Lee C., Hsiao W. Optimizing piezoelectric transformer for maximum power transfer. Smart Material and Structures, 2003. P. 373–383. https://doi.org/10.1088/0964-1726/12/3/308
11. Kakehashi H., Hidaka T., Ninomiya T., Shoyama M., Ogasawara H., Ohta Y. Electronic ballast using piezoelectric transformers for fluorescent lamps, in Proc. IEEE APEC, 1998. P. 29–35.
12. Yang J. Piezoelectric transformer structural modeling – a review, IEEE Transactions on Ultrasonics, Ferroelectrics, and Frequency Control. 2007. 54 (6). P. 1154–1170. https://doi.org/10.1109/TUFFC.2007.369
13. Hemsel T., Priya S. Model based analysis of piezoelectric transformers, Ultrasonics, 2006, 44, Supplement, e741-e745. https://doi.org/10.1016/j.ultras.2006.05.086
14. Pulpan P., Erhart J. & Štípek O. Analytical Modeling of Piezoelectric Transformers, Ferroelectrics, 2007, 351 (1). P. 204–215. https://doi.org/10.1080/00150190701354299
15. Ivensky G.; Zafrany I. and Ben-Yaakov S. General operation characteristics of piezoelectric transformers, IEEE Trans. Power Electron. 2002. 17 (6). P. 1049–1057. https://doi.org/10.1109/TPEL.2002.805602
16. Bolborici V., Dawson F. P., Pugh M. C. Modeling of composite piezoelectric structures with the finite volume method, IEEE Transactions on Ultrasonics, Ferroelectrics and Frequency Control. 2012. 59 (1). P. 156–162. https://doi.org/10.1109/TUFFC.2012.2167

**Список використаних джерел**
1. Katz H. W. Solid state magnetic and dielectric devices. New York: Wiley, 1959. 542 p.
2. Лавриненко В. В. Пьезоэлектрические трансформаторы. М.: Энергия, 1975. 112 с.
3. Yang Y. J., Chen C. C., Chen Y. M., et al., Modeling of piezoelectric transformers using finite-element technique. Journal of the Chinese Institute of Engineers. 2008. 31 (6). P. 925–932. https://doi.org/10.1080/02533839.2008.9671447
4. Ерофеев А. А., Данов Г. А., Флоров В. Н. Пьезокерамические трансформаторы и их применение в радиоэлектронике. М.: Радио и связь, 1988. 128 с.
5. Harris J. W., Horst S. Handbook of mathematics and computational science. Springer Science & Business Media, 1998. https://doi.org/10.1007/978-1-4612-5317-4
6. Ерофеев А. А., Пьезоэлектронные устройства автоматики Piezoelectronic automation devices. Leningrad: Mashinostroenie, 1982. 212 p.
7. Vazquez Carazo, A. Piezoelectric Transformers: An Historical Review. Actuators 2016, 5, 12. Doi: 10.3390/act5020012. https://doi.org/10.3390/act5020012
8. Ozeri S. and Shmilovitz D. Piezoelectric transformers model parameters extraction based on time domain measurements, Twenty-First Annual IEEE Applied Power Electronics Conference and Exposition, 2006. APEC '06., 2006. P. 5. Doi: 10.1109/APEC.2006.1620748.
9. Bronshtein S., Abramovitz A., Bronshtein A. and Katz I. A Method for Parameter Extraction of Piezoelectric Transformers. IEEE Transactions on Power Electronics. 2011. 26 (11). P. 3395–3401. https://doi.org/10.1109/TPEL.2011.2139225
10. Hsu Y., Lee C., Hsiao W. Optimizing piezoelectric transformer for maximum power transfer. Smart Material and Structures, 2003. P. 373–383. https://doi.org/10.1088/0964-1726/12/3/308
11. Kakehashi H., Hidaka T., Ninomiya T., Shoyama M., Ogasawara H., Ohta Y. Electronic ballast using piezoelectric transformers for fluorescent lamps, in Proc. IEEE APEC, 1998. P. 29–35.
12. Yang J. Piezoelectric transformer structural modeling – a review, IEEE Transactions on Ultrasonics, Ferroelectrics, and Frequency Control. 2007. 54 (6). P. 1154–1170. https://doi.org/10.1109/TUFFC.2007.369
13. Hemsel T., Priya S. Model based analysis of piezoelectric transformers, Ultrasonics, 2006, 44, Supplement, e741-e745. https://doi.org/10.1016/j.ultras.2006.05.086
14. Pulpan P., Erhart J. & Štípek O. Analytical Modeling of Piezoelectric Transformers, Ferroelectrics, 2007, 351 (1). P. 204–215. https://doi.org/10.1080/00150190701354299
15. Ivensky G.; Zafrany I. and Ben-Yaakov S. General operation characteristics of piezoelectric transformers, IEEE Trans. Power Electron. 2002. 17 (6). P. 1049–1057. https://doi.org/10.1109/TPEL.2002.805602

16. Bolborici V., Dawson F. P., Pugh M. C. Modeling of composite piezoelectric structures with the finite volume method, IEEE Transactions on Ultrasonics, Ferroelectrics and Frequency Control. 2012. 59 (1). P. 156–162. https://doi.org/10.1109/TUFFC.2012.2167

УДК 681.586

# ОДНОВИМІРНА МАТЕМАТИЧНА МОДЕЛЬ П'ЄЗОЕЛЕКТРИЧНИХ ТРАНСФОРМАТОРІВ ДЛЯ СИСТЕМИ САПР

## Володимир Медвідь; Ірина Белякова; Олена Марущак; Вадим Пісьціо

*Тернопільський національний технічний університет імені Івана Пулюя, Тернопіль, Україна*

*Резюме. Представлено модель п'єзоелектричного трансформатора (ПТ), зручніша для моделювання в порівнянні з тими, які широко застосовуються на практиці. Отримано аналітичні вирази для побудови наближеної одномірної моделі п'єзотрансформатора, котра значно простіша, ніж скінчено-елементна модель. Також, на відміну від класичної моделі, запропонована схема та метод моделювання дають змогу врахувати наявність ділянок з поздовжньою або поперечною поляризацією, довільне їх сполучення та взаємне розміщення. На основі описаної методики моделювання запропоновано схему моделювання окремої ділянки п'єзоелемента як одного багатополюсника. За допомогою відповідного з'єднання таких багатополюсників, кожен з котрих має власний розподіл електродів та власні геометричні параметри, може бути отримано необхідний п'єзоелектричний трансформатор. Тобто, наведена модель дозволяє створити п'єзоелектричний трансформатор як схему, що складається зі стандартних блоків, що спрощує розташування електродів і узгодження зі схемою. Також запропонована модель враховує будь-яку кількість резонансів і наявність кількох електродів, розташованих на п'єзоелектричному трансформаторі. Крім того, запропонована модель може бути безпосередньо застосована при розробленні радіоелектронного обладнання та інтегрована в системи автоматизованого проектування (САПР). На прикладі показано реалізацію цієї моделі в системі автоматизованого проектування MicroCAP. Для підтвердження розвинених теоретичних представлень побудовано модульну модель ПТ у САРП MicroCAP та проведено порівняння отриманих розрахункових даних із експериментальними.*

*Ключові слова: Схема заміщення, п'єзоелектричний трансформатор, п'єзоелемент, частотні гармоніки, MicroCAP.*